Mechanisms of Substitution Reactions on Cyclometallated Platinum(IV) Complexes: "Quasi-labile" Systems

Paul V. Bernhardt,[†] Carlos Gallego,[‡] and Manuel Martinez*,[‡]

Department of Chemistry, University of Queensland, Brisbane 4072, Australia, and Departament de Química Inorgànica, Universitat de Barcelona, Martí i Franquès 1-11, E-08028 Barcelona, Spain

Received June 16, 2000

The substitution reactions of SMe_2 by phosphines ($PMePh_2$, $PEtPh_2$, PPh_3, $P(4\text{-}MeC_6H_4)_3$, $P(3\text{-}MeC_6H_4)_3$, PCy_3) on Pt^{IV} complexes having a cyclometalated imine ligand, two methyl groups in a *cis*-geometrical arrangement, a halogen, and a dimethyl sulfide as ligands, $[Pt(C\frown N)(CH_3)_2(X)(SMe_2)]$, have been studied as a function of temperature, solvent, and electronic and steric characteristics of the phosphines and the X and C⁀N ligands. In all cases, a limiting dissociative mechanism has been found, where the dissociation of the SMe_2 ligand corresponds to the rate-determining step. The pentacoordinated species formed behaves as a true pentacoordinated Pt^{IV} compound in a steady-state concentration, given the solvent independence of the rate constant. The X-ray crystal structures of two of the dimethyl sulfide complexes and a derivative of the pentacoordinate intermediate have been determined. Differences in the individual rate constants for the entrance of the phosphine ligand can only be estimated as reactivity ratios. In all cases an effect of the phosphine size is detected, indicating that an associative step takes place from the pentacoordinated intermediate. The nature of the C⁀N imine and X ligands produces differences in the dimethyl sulfide dissociation reactions rates, which can be quantified by the corresponding $\Delta S^{\ddagger}$ values (72, 64, 48, 31, and 78 J K^{-1} mol^{-1} for C⁀N/X being $C_6H_4CHNCH_2C_6H_5$/Br, $C_6H_4CHNCH_2$-(2,4,6-$(CH_3)_3$)C_6H_2/Br, $C_6H_4CHNCH_2C_6H_5$/Cl, $C_6Cl_4CHNCH_2C_6H_5$/Cl, and $C_6H_4CH_2NCHC_6H_5$/Br, respectively). As a whole, the donor character of the coordinated $C^{aromatic}$ and X atoms have the greatest influence on the dissociativeness of the rate-determining step.

Introduction

The study of substitution reactions on Pt^{IV} complexes has always been elusive, despite the inherent inertness associated with its t_{2g}^6 electronic configuration.[1] For Werner-type complexes, the presence of redox-assisted processes has, in fact, prevented its proper study.[2] In the case of organometallic complexes this effect can be more easily avoided; nevertheless, very little information is available about rate constants and substitution mechanisms for these type of complexes.[3] In any case, it is clear that the presence of a large number of Pt−C bonds produces a tendency both toward more dissociatively activated substitution mechanisms[4] and to more labile complexes, given the larger electron density at the metal center (i.e., Pt^{II} resembles Pt^0, and Pt^{IV} resembles Pt^{II}).[5] Some important studies have been carried out with square-planar Pt^{II} complexes,[6] and the results obtained have been interpreted in the same context. Historically, Pt^{IV} organometallic chemistry has generally involved oxidative addition−reductive elimination reactions (and their derivative processes);[7] furthermore, a number of hydrido Pt^{IV} complexes have appeared recently.[8] Pt^{IV} to Pt^{II} reduction processes have lately also been attracting much attention, given the nature of the new generation of anticancer platinum pharmaceuticals.[9] In any of these processes the initial substitution reaction is crucial, but poorly understood.

We have been involved in the mechanistic studies of imine cyclometalation reactions via oxidative additions at Pt^{II} centers. In these processes, a final fast association of SMe_2 to the coordination sphere to produce the final compounds is assumed.[10a−d]

[†] University of Queensland.
[‡] Universitat de Barcelona.

(1) (a) Tobe, M. L.; Burgess, J. *Inorganic Reaction Mechanisms*; Longman: Essex, U.K., 1999. (b) Dixon, N. E.; Lawrance, G. A.; Lay, P. A.; Sargeson, A. M. *Inorg. Chem.* **1983**, *22*, 846. (c) Curtis, N. J.; Lawrance, G. A.; Lay, P. A.; Sargeson, A. M. *Inorg. Chem.* **1986**, *25*, 484.

(2) Peloso, A. *Coord. Chem. Rev.* **1973**, *10*, 123.

(3) (a) Lashanizadehgan, M.; Rashidi, M.; Hux, J. E.; Puddephatt, R. J.; Ling, S. S. M. *J. Organomet. Chem.* **1984**, *269*, 317. (b) Hux, J. E.; Puddephatt, R. J. *Inorg. Chim. Acta* **1985**, *100*, 1.

(4) (a) Frey, U.; Helm, L.; Merbach, A. E.; Romeo, R. *J. Am. Chem. Soc.* **1989**, *111*, 8161.

(5) Romeo, R. *Comments Inorg. Chem.* **1990**, *11*, 21.

(6) (a) Elmroth, S.; Bugarcic, Z.; Elding, L. I. *Inorg. Chem.* **1992**, *31*, 3551. (b) Romeo, R.; Scolaro, L. M.; Nastasi, N.; Arena, G. *Inorg. Chem.* **1996**, *35*, 5087. (c) Wendt, O. F.; Elding, L. I. *Inorg. Chem.* **1997**, *36*, 6028. (d) Schmülling, M.; van Eldik, R. *Chem. Ber./Recl.* **1997**, *130*, 17−91.

(7) (a) Wick, D. D.; Goldberg, K. I. *J. Am. Chem. Soc.* **1997**, *119*, 10235. (b) Baar, C. R.; Hill, G. S.; Vittal, J. J.; Puddephatt, R. J. *Organometallics* **1998**, *17*, 32.

(8) Jenkins, H. A.; Yap, G. P. A.; Puddephatt, R. J. *Organometallics* **1997**, *16*, 1946.

(9) (a) Shi, T.; Berglund, J.; Elding, L. I. *Inorg. Chem.*, **1996**, *35*, 3498. (b) Choi, S.; Mahalinggaiah, S.; Delaney, S.; Neale, N. R.; Massod, S. *Inorg. Chem.* **1999**, *38*, 1800.

10.1021/om000505y CCC: $19.00
Publication on Web 10/21/2000

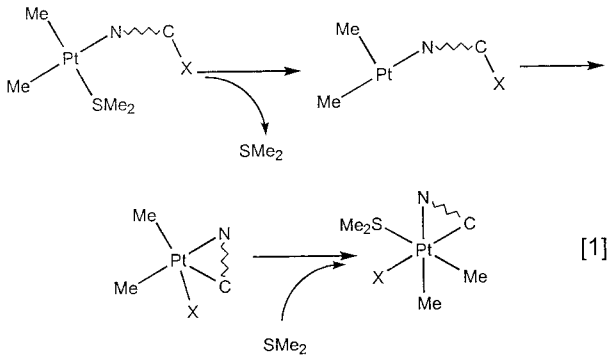

[1]

Full X-ray characterization of the final dimethyl sulfide cyclometalated compounds had proved elusive, but further reaction of the derivative of imine 2-ClC_6H_4-$CHNCH_2C_6H_5$ with PPh_3 produced the corresponding phosphine derivative. The structure of this compound has a *trans*XC^{arm} isomeric form (**2d**χ, Scheme 1).[10a] The assumed lability of the Pt−S bond has attracted our attention, given its supposed inertness. In fact, the interchange of the methyl groups in oxidative addition reactions of MeI in this type of complexes[12] has already suggested its fast substitution reactivity. Recent kinetic studies have also confirmed that dimethyl sulfide substitution reaction rates are quite fast.[13]

In this paper we present the X-ray crystal structure determination of two dimethyl sulfide complexes, **1a** and **1e**, depicted in Scheme 1, and the study of the kinetics and mechanism for the reaction of **1a**, **1b**, **1c**, **1e**, and **1f** with phosphines, of varying electronic and steric characteristics, in different solvents and at different temperatures, to produce the corresponding compounds **2**. The crystal structure of a dimeric form of the cyclometalated compound **1f**, **1f2**, has also been determined, proving the feasibility of the existence a pentacoordinate intermediate during the reaction process. The variation of entering ligand characteristics and the different electronic and steric factors of the inert ligands C⁀N and X allow us to examine the factors that are dominant in substitution reactions of these types of organometallic Pt^{IV} complexes.

Results and Discussion

It has previously been assumed that, given its concerted nature, the oxidative addition process (eq 1) of imines at Pt^{II} centers produces the *cis*XC^{arm} isomers of the Pt^{IV} dimethyl sulfide cyclometalated compounds and that further reaction with phosphines effects isomerization to the less sterically demanding *trans*XC^{arm} isomer (**2**).[10a] Nevertheless, the implied and observed lability of the SMe_2 ligand in this type of organometallic complexes brought in a certain degree of incoherence in the results. We have now managed to isolate X-ray quality crystals of Pt^{IV} compounds with imines **a** and **d** and SMe_2 ligand, and their structures have been determined (Tables 1 and 2, and Figure 1a,b) (Tables S1−S10, Supporting Information). The geometrical arrangement around the Pt^{IV} center agrees with that of the established[10] phosphine derivatives (*cis*-Me_2 *trans*XC^{arm}). That is, the isomerization process does not occur during the phosphine substitution process but during the final step of the oxidative addition reaction (eq 1). The consequence is that the pentacoordinate intermediate produced after the concerted C−X oxidative addition on the Pt^{II} center lives long enough to rearrange from a *cis*XC^{arm} geometrical arrangement to the most stable *trans*XC^{arm}, which is that found in the structures of both the dimethyl sulfide and phosphine derivatives determined (**1a**, **1e**, **2d**χ). In this respect, the isolation of the dimeric complex **1f2** (Tables 1 and 2, and Figure 1c) (Tables S11−S15, Supporting Information) from long standing dilute solutions of compound **1f** establishes the existence of such a pentacoordinate species in solution, although in very low concentrations.

2D NOESY ^{1}H NMR experiments in acetone solution at room temperature of compounds **1b** and **1e** show that interchange of the two *cis*-methyl groups takes place in less than 2−3 s at room temperature. It seems that a "quasi-lability" of the SMe_2 ligands enables an important reorganization from the pentacoordinate intermediate (trigonal bipyramid turnstile twist)[14] in a way that

Scheme 1

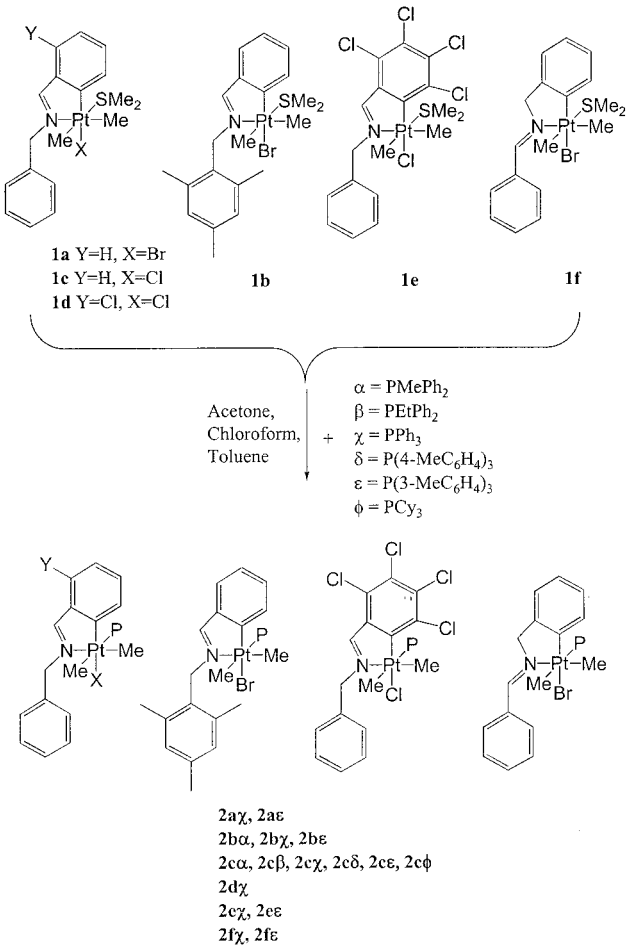

(10) (a) Crespo, M.; Martinez, M.; Sales, J.; Solans, X.; Font-Bardia, M. *Organometallics* **1992**, *11*, 1288. (b) Crespo, M.; Martinez, M.; Sales, J. *J. Chem. Soc., Chem. Commun.* **1992**, 822. (c) Crespo, M.; Martinez, M.; Sales, J. *Organometallics* **1993**, *12*, 429−7. (d) Crespo, M.; Martinez, M.; de Pablo, E. *J. Chem. Soc., Dalton Trans.* **1997**, 1321.

(11) Anderson, C. M.; Crespo, M.; Jennings, M. C.; Lough, A. L.; Ferguson, G.; Puddephatt, R. J. *Organometallics* **1991**, *10*, 2672.

(12) Crespo, M.; Puddephatt, R. J. *Organometallics* **1987**, *6*, 2548.

(13) (a) Nakayama, K.; Kondo, Y.; Ishihara, K. *Can. J. Chem.* **1998**, *76*, 62. (b) Kondo, Y.; Oda, Y.; Ishihara, K. *Int. J. Chem. Kinet.* **1998**, *30*, 523.

(14) Ugi, I.; Ramirez, F.; Marquarding, D.; Klusacek, H.; Gokel, G.; Guillespie, P. *Angew. Chem., Int. Ed. Engl.* **1970**, *9*, 7−03.

Table 1. Crystal Data

	1a	**1e**·$^1/_2$Me$_2$CO	**1f2**
space group	*Cc* (No. 9)	$P\bar{1}$ (No. 2)	*C*2/*c* (No. 15)
formula	$C_{18}H_{24}BrNPtS$	$C_{19.5}H_{23}Cl_5NO_{0.5}PtS$	$C_{32}H_{36}Br_2N_2Pt_2$
a, Å	20.046(4)	8.723(2)	34.90(1)
b, Å	7.569(1)	11.626(2)	11.163(2)
c, Å	13.649(4)	12.571(2)	15.760(8)
α, deg		107.61(2)	
β, deg	112.15(1)	99.29(2)	94.64(2)
γ, deg		93.23(2)	
V, Å^3	1918.1(7)	1191.7(4)	6120(4)
ρ_{calc}, g cm^{-3}	1.944	1.906	2.168
fw	561.44	683.79	998.63
Z	4	2	8
μ, cm^{-1}	95.04	65.45	117.69
temp, K	293	293	293
λ, Å	0.71073	0.71073	0.71073
N	1737	4185	5381
N_o ($F_o > 2\sigma$)	1657	3812	2451
$2\theta_{max}$, deg	50	50	50
$R(F_o)$, $wR_2(F_o^2)$	0.0204,0.0516	0.0327, 0.0861	0.0501, 0.1019

Table 2. Relevant Bond Angles and Distances for the Crystal Structures Depicted in Figure 1

bond length /Å	**1a** (X = Br)	**1e** (X = Cl)	**1f2** (X = Br)	bond angle/deg	**1a** (X = Br)	**1e** (X = Cl)	**1f2** (X = Br)
Pt1−S1	2.441(2)	2.469(2)		X1−Pt1−S1	85.44(8)	90.75(6)	
Pt1−X1	2.569(1)	2.388(2)	2.632(2)	C3−Pt1−S1	94.8(2)	90.2(2)	
Pt1−X2			2.633(2)	C1−Pt1−S1	86.6(4)	93.1(2)	
Pt2−X1			2.678(2)	N1−Pt1−S1	93.6(2)	96.04(14)	
Pt2−X2			2.607(2)	C1−Pt1−X1	84.4(4)	87.5(2)	
Pt1−N1	2.163(7)	2.149(5)		C1A−Pt1−X1			87.5(6)
Pt1−N1A			2.193(14)	C1A−Pt1−X2			89.2(5)
Pt2−N1B			2.193(14)	C1B−Pt2−X1			89.0(6)
Pt1−C1	2.063(11)	2.071(6)		C1B−Pt2−X2			85.9(6)
Pt1−C1A			2.016(18)	N1−Pt1−X1	95.2(2)	92.52(14)	
Pt2−C1B			2.020(19)	N1A−Pt1−X1			97.5(4)
Pt1−C2	2.071(9)	2.065(6)		N1A−Pt1−X2			87.3(4)
Pt1−C2A			2.029(16)	N1B−Pt2−X1			87.6(4)
Pt2−C2B			2.043(17)	N1B−Pt2−X2			99.0(4)
Pt1−C3	1.996(8)	2.033(6)		S1−Pt1−C2	172.6(3)	177.04(19)	
Pt1−C3A			1.960(19)	X1−Pt1−C2	90.5(3)	90.6(2)	
Pt2−C3B			2.020(20)	X1−Pt1−C2A			96.8(5)
				X2−Pt1−C2A			178.0(5)
				X1−Pt2−C2B			176.7(6)
				X2−Pt2−C2B			94.9(6)
				C3−Pt1−C2	89.8(4)	88.9(3)	
				C3A−Pt1−C2A			86.7(7)
				C3B−Pt2−C2B			88.0(8)
				C1−Pt1−C2	87.3(5)	84.3(3)	
				C1A−Pt1−C2A			88.8(7)
				C1B−Pt2−C2B			88.2(8)
				N1−Pt1−C2	92.9(3)	86.5(3)	
				N1A−Pt1−C2A			94.6(6)
				N1B−Pt2−C2B			80.3(8)
				C1−Pt1−C3	94.1(4)	99.9(3)	
				C1A−Pt1−C3A			94.8(8)
				C1B−Pt2−C3B			94.6(9)
				N1−Pt1−C3	79.9(3)	80.0(2)	
				N1A−Pt1−C3A			80.0(7)
				N1B−Pt1−C3B			80.3(8)

only the most stable geometrical arrangement of the complex is the dominant species in solution, i.e., the *cis*-Me_2, *trans*XC^{arm} form. The UV−vis monitoring of the phosphine substitution reaction on complexes **1a**, **1b**, **1c**, **1e**, and **1f** in different solvents has been pursued in order to establish the nature of this lower coordination number intermediate. When the 2D NOESY experiment is run on the phosphine derivative **2e***χ* complex, no interchange of the *cis*-methyl groups is observed on the same time scale, which is consistent with the observed irreversible character of these substitution reactions under the reaction conditions studied. In the absence of free PPh_3, the reaction of compounds **2c***χ* and **2e***χ* with SMe_2 in acetone solution has been monitored by ^{1}H NMR. Although the reaction takes place, only ca. 20% and 35%, respectively, of the dimethyl sulfide derivative is produced over a period of 24 h at room temperature. When pseudo-first-order conditions of phosphine and dimethyl sulfide are applied, no phosphine substitution by dimethyl sulfide is observed, as shown by ^{1}H NMR.

^{31}P and ^{1}H NMR monitoring of the products of the reactions under the same conditions indicate that the process is clean; this is confirmed by the observation of isosbestic points in the UV−vis spectra over time. In the absence of added SMe_2, the reaction rate constant is independent of the phosphine concentration, while an important retardation effect is detected in the presence

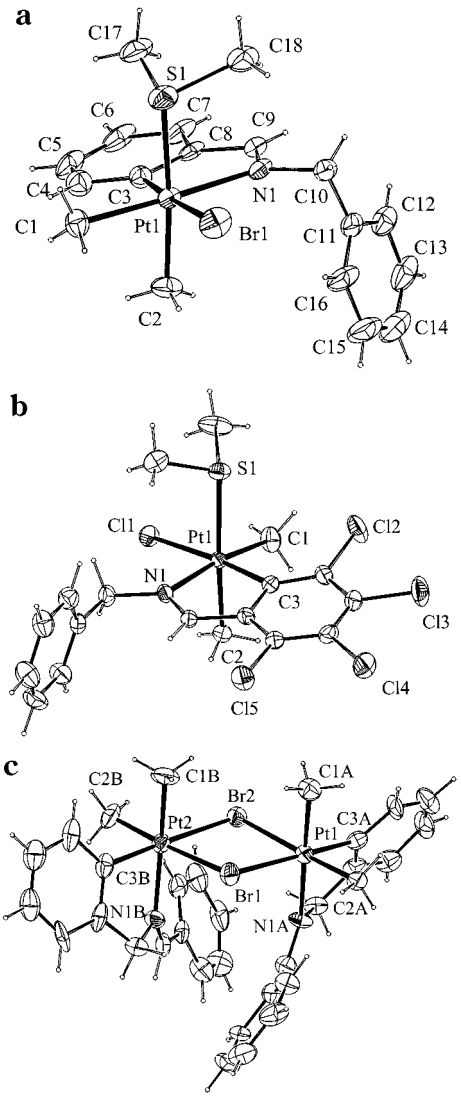

Figure 1. View of the complexes (a) **1a**, (b) **1e**, and (c) **1f2**. Ellipsoids indicate 30% probability.

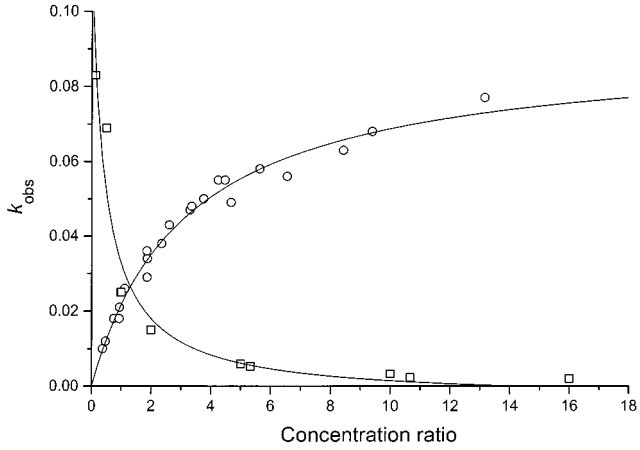

Figure 2. Plots of 10 × $k_{obs}(s^{-1})$ versus $[SMe_2]/[PCy_3]$ (eq 3) at 10 °C (□) and $k_{obs}(s^{-1})$ versus $[PPh_3]/[SMe_2]$ (eq 4) at 20 °C (○) for compound **1c** in acetone solution.

of dimethyl sulfide, with a concomitant dependence on the concentration of phosphine. Figure 2 illustrates the dependence of k_{obs} on the ratios $[SMe_2]/[phosphine]$ and $[phosphine]/[SMe_2]$ for two of the systems studied. As indicated for similar systems,[15] the following reaction

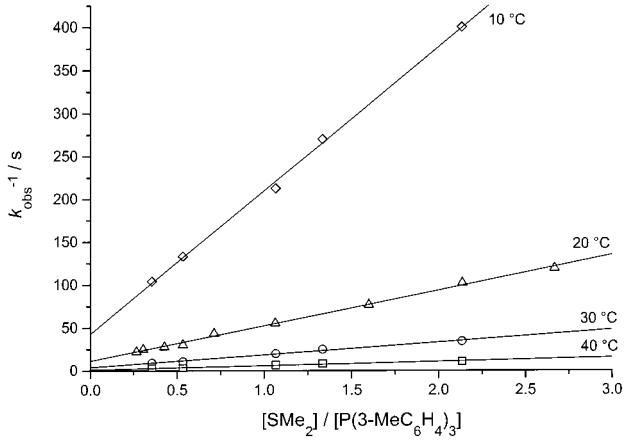

Figure 3. Plot of $1/k_{obs}$ versus $[SMe_2]/[P(3\text{-}MeC_6H_4)_3]$ for the substitution of dimethyl sulfide on compound **1c** in acetone solution.

Scheme 2

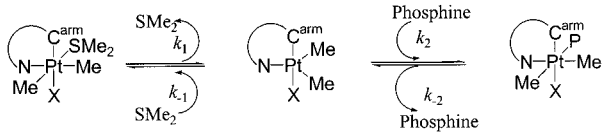

scheme (Scheme 2) and rate law (eqs 2−4) are obtained, once the steady-state approximation is assumed for a pentacoordinate intermediate.[16]

$$k_{obs} = \frac{k_1k_2[\text{Phoshine}] + k_{-1}k_{-2}[SMe_2]}{(k_{-1}[SMe_2] + k_2[\text{Phosphine}])} \qquad [2]$$

$$k_{obs} = \frac{k_1k_2 + k_{-1}k_{-2}([SMe_2]/[\text{Phoshine}])}{(k_{-1}([SMe_2]/[\text{Phoshine}]) + k_2)}$$

$\longrightarrow k_{-2}$ at large $[SMe_2]/[\text{Phoshine}]$ values [3]

$$k_{obs} = \frac{k_1k_2([\text{Phoshine}]/[SMe_2]) + k_{-1}k_2}{(k_{-1} + k_2([\text{Phosphine}]/[SMe_2]))}$$

$\longrightarrow k_1$ at large $[\text{Phoshine}]/[SMe_2]$ values [4]

Although in some cases very small values for k_{-2} can be estimated, their significance and reproducibility with changes in temperature are very small, making them impossible to evaluate. On the contrary, the limiting value for k_1 is easily evaluated, and eq 4 can be transformed in eqs 5 and 6.

$$k_{obs} = \frac{k_1k_2[\text{Phoshine}]}{(k_{-1}[SMe_2] + k_2[\text{Phosphine}])} \qquad [5]$$

$$\{1/k_{obs}\} = \{1/k_1\} + \{k_{-1}/(k_1k_2)\} \times \{[SMe_2]/[\text{Phosphine}]\} \qquad [6]$$

From the plots of $1/k_{obs}$ versus $[SMe_2]/[\text{phosphine}]$ (eq 6) the values of k_1, K_1k_2 ($K_1 = k_1/k_{-1}$), and the k_{-1}/k_2 ratio for all the systems studied can be determined (Figure 3).

The values of K_1k_2 derived directly from the slopes of the plot of eq 3, and their associated thermal activation parameters, are revealing. Taking into account that the value of K_1 should be the same for a given compound **1**, their differences for each compound have to be solely

(15) Basallote, M. G.; Durán, J.; Fernández-Trujillo, M.-J.; Máñez, M.-A. *J. Chem. Soc., Dalton Trans.* **1998**, 3227.
(16) Espenson, J. H. *Chemical Kinetics and Reaction Mechanisms*, 2nd ed.; McGraw-Hill: New York, 1995.

Table 3. Kinetic and Thermal Activation Parameters for K_1k_2 for the Reactions Studied ([Pt] = 2.5 × 10^{-4} M, [Phosphine] > 25 × 10^{-4} M, [SMe_2] > 25 × 10^{-4} M)

compound	phosphine	solvent	$10^2 \times K_1k_2$[a]/M s^{-1}	$\Delta H^{\ddagger}$/kJ mol^{-1}	$\Delta S^{\ddagger}$/J K^{-1} mol^{-1}
1a	χ	acetone	5.4	81 ± 5	2 ± 17
		chloroform	4.7	95 ± 10	46 ± 35
		toluene	6.3	89 ± 5	24 ± 16
	ϵ	acetone	4.9	94 ± 7	45 ± 25
		toluene	4.6	91 ± 3	32 ± 10
1b	α	acetone	5.4	98 ± 2	57 ± 7
	χ	acetone	2.4	83 ± 2	2 ± 8
		chloroform	1.8	82 ± 3	−4 ± 9
	ϵ	acetone	1.6	93 ± 3	31 ± 10
1c	α	acetone	7.6	86 ± 6	21 ± 22
	β	acetone	7.3	89 ± 5	29 ± 18
	χ	acetone	5.1	88 ± 2	24 ± 8
	δ	acetone	4.2	77 ± 5	−16 ± 16
	ϵ	acetone	4.0	84 ± 3	9 ± 8
	ϕ	acetone	3.0	110 ± 8	93 ± 28
1e	χ	acetone	4.8	86 ± 5	16 ± 17
		chloroform	4.2	88 ± 8	24 ± 29
	ϵ	acetone	4.0	95 ± 4	44 ± 12
		chloroform	3.2	83 ± 9	4 ± 31
1f	χ	acetone	5.4	105 ± 6	81 ± 19
	ϵ	acetone	3.7	100 ± 10	60 ± 34

[a] Extrapolated from Eyring plots at 298 K. From ref 17a: $PMePh_2$, α, $pK_a = 4.06$, $\theta = 136°$; $PEtPh_2$, β, $pK_a = 4.6$, $\theta = 140°$; PPh_3, χ, $pK_a = 3.28$, $\theta = 145°$; $P(4\text{-}MeC_6H_4)_3$, δ, $pK_a = 4.46$, $\theta = 145°$; $P(3\text{-}MeC_6H_4)_3$, ϵ, $pK_a = 4.7$, $\theta = 165°$; PCy_3, ϕ, $pK_a = 11.26$, $\theta = 170°$.

related to changes in k_2. Table 3 shows the thermal kinetic parameters derived from the corresponding Eyring plots for all the systems studied, together with the interpolated value of K_1k_2 at 298 K. For any of the substitutions of dimethyl sulfide by phosphines on the cyclometalated systems studied, enthalpies are in a very narrow margin, while entropies, although more scattered due to their inherent errors, are close to zero or slightly positive. Considering that ΔS^0 for K_1 is bound to be extremely positive, $\Delta S^{\ddagger}(k_2)$ has to be very negative, as expected for an associatively activated process as that depicted in Scheme 2. For the *endo* cyclometalated complexes, only $\Delta S^{\ddagger}$ for the **1c** plus ϕ system is significantly more positive, indicating that the degree of ordering in the transition state for k_2 is less than for the rest of the studied phosphine substitution reactions. Steric reasons can be held responsible for the lesser degree of association in the transition state. In this respect, no substitution reaction has been detected, by ^{31}P NMR, for compounds of the **1** series with the bulky $P(2\text{-}MeC_6H_4)_3$ phosphine; a cone angle of 194° seems to be far too large for the process to occur. For the *exo* cyclometalated **1f** plus χ and ϵ systems, the values collected in Table 3 for $\Delta S^{\ddagger}$ are as a whole more positive, indicating a lesser ordering in the transition state; the rigidity of the benzylidene residue of the cyclometalated ligand can be easily related with this fact. The isolation of compound **1f2** also agrees with the fact that the pentacoordinate intermediate keeps a fairly open structure. With reference to $\Delta H^{\ddagger}$ for the different systems studied, and taking into account the expected different values for $\Delta H^0(K_1)$, the results are surprising. Considering that differences in $\Delta H^0(K_1)$ are composite, and that they can be easily compensated by $\Delta H^{\ddagger}(k_2)$, any further discussion seems fruitless.

From Scheme 2, the values of k_1, determined from the intercepts of eq 6, are expected to be independent of the steric and electronic characteristics of the entering phosphine ligands; furthermore, if the nature of the pentacoordinated intermediate is that depicted, they should also be independent of the solvents used. Figure 4 shows such independence for all the studied systems, allowing the entropies and enthalpies of activation to be derived from these global Eyring plots. The values

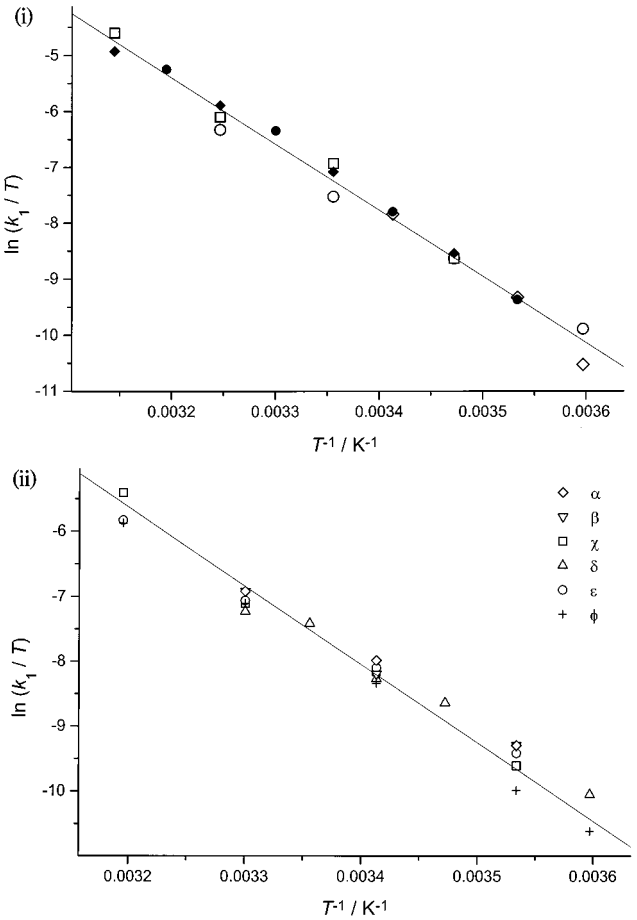

Figure 4. (i) Eyring plot for the value of k_1 for the reaction of compound **1a** with phosphines χ (PPh_3, empty points) and ϵ ($P(3\text{-}MeC_6H_4)_3$, solid points) in the different solvents used (○, acetone; □, chloroform; ◇, toluene). (ii) Eyring plot for the value of k_1 for the reaction of compound **1c** with different phosphines in acetone solution.

Table 4. Average Kinetic and Thermal Activation Parameters for Rate Constant k_1 for the Reactions Studied ([Pt] = 2.5 × 10^{-4} M, [Phosphine] > 25 × 10^{-4} M, [SMe$_2$] > 25 × 10^{-4} M)

compound	phosphine	solvent	k_1[a]/s^{-1}	$\Delta H^{\ddagger}$/kJ mol^{-1}	$\Delta S^{\ddagger}$/J K^{-1} mol^{-1}
1a	χ, ϵ	acetone, chloroform, toluene	0.21	99 ± 3	72 ± 9
1b	α, χ, ϵ	acetone, chloroform	0.062	99 ± 5	64 ± 15
1c	α, β, χ, δ, ϵ, ϕ	acetone	0.15	92 ± 3	48 ± 10
1e	χ, ϵ	acetone, chloroform	0.040	91 ± 3	31 ± 10
1f	χ, ϵ	acetone	0.34	99 ± 4	78 ± 13

[a] Extrapolated from Eyring plots at 298 K.

calculated for these parameters, as a function of the inert Pt^{IV} organometallic skeleton, are collected in Table 4, together with the interpolated k_1 values at 298 K. It is important to note the large intrinsic errors involved in the individual determination of k_1 for the different systems; given the fact that the intercepts of the plots depicted by eq 6 are close to zero, small differences in the individual values found for these rate constants should not be considered as significant. Plots such as the one shown in Figure 4 tend to statistically cancel these errors, making any differences in the thermal activation parameters much more reliable. From plots such as Figure 4i, and considering the important differences in the standard parameters of the solvents used (dielectric constant, polarity, refraction index, viscosity),[18] it seems clear that the transition state leading to the species with a lower coordination number depicted in Scheme 2 is independent of the solvent characteristics. This fact indicates that such a species is a true pentacoordinated intermediate with no influence of the solvent on the coordination sphere of the Pt^{IV} center, as evidenced by the K_1k_2 parameters. The only measurable effect on the reaction rate and activation parameters in this series should then be related with steric and electronic influences on the dissociating Pt−SMe$_2$ bond. In this respect, the homogeneity of values determined for $\Delta H^{\ddagger}$ is remarkable taking into account the important differences expected for the strength of the Pt−SMe$_2$ bond. Although the electronic differences between compounds **1a**, **1b**, and **1c** can be argued to be very small, compound **1e** represents a very important change in the electronic influence on the Pt−C^{aromatic} bond, while retaining the same Pt−X moiety as compound **1c**. Furthermore, although the Pt−X bonds are the same for the three complexes **1a**, **1b**, and **1f**, variations in the steric demands of the cyclometalated compound might be important. Probably the large σ-donor character of the labilizing *trans*-methyl group on the dissociating SMe$_2$ is responsible for this homogeneity. Given the fact that, as seen in Table 4, the differences in the reactivity for these processes seem to be solely related with the activation entropy, the degree of dissociativeness or disorder in the transition state has to play a key role.

From the data collected, the degree of disorder seems to be at a maximum for compounds **1a** and **1f** and at a minimum for compound **1e**. Comparison of the data in pairs of complexes, where only one change in the cyclometallating or X ligands is present, is much more revealing. While for compound **1a** the activation entropy is +72 J K^{-1} mol^{-1}, when the Br ligand is substituted by Cl (compound **1c**), a decrease in dissociativeness is achieved, indicated by a decrease to +48 J K^{-1} mol^{-1} in the value of $\Delta S^{\ddagger}$. Although the errors are large, the trend is significant. Both electronic and steric factors can be held responsible for this fact; decreasing the size of X and increasing its electronegativity, while keeping the same value of activation enthalpy to reach the transition state, disfavors dissociation of the SMe$_2$ ligand in compounds of the **1** series. That is, the transition state should be in a more advanced position along the reaction coordinate for compound **1a** with respect to **1c**. Differences between the values for compounds **1a** and **1b** are less important, as expected for the very small differences between the two cyclometalated imine ligands. The steric demands of compound **1b** do not produce an increased dissociation on the transition state, probably due to the wrapping effect of the mesityl group attached to the imine N, when compared with compound **1a**. The differences between the thermal activation parameters for compounds **1c** and **1e** also suggest a decrease in the degree of dissociativenes on changing from a perchloro to an unsubstituted metalated ring. In this case, the effect has to be electronic, given the obviously minor effect of the metalated ring substituents in the hindrance on the Pt−SMe$_2$ bond. As indicated above, and considering that the enthalpy barrier is the same, the lesser electron density around the metal for the perchloro compound, **1e**, should force a lesser degree of dissociation than that for compound **1c** in the transition state of the reaction. Finally comparison of the **1a** and **1f** data indicates that any aromaticity present on the *endo* **1a** compound[19] does not affect the electron density on the Pt^{IV} center and, thus, has no effect on the SMe$_2$ dissociation; in fact, ^{195}Pt NMR of compounds **1a** and **1f** show a signal at −2373 ppm (acetone d_6, reference H$_2$[PtCl$_6$]) in both cases, in good agreement with the results indicated above. Changes in flexibility of the cyclometalated dangling arm do not seem to affect the activation parameters for the dissociative process (k_1), contrary to what has been found for the associative process (K_1k_2).

Examination of the bonding data of the available crystal structures for a compound of type **1** (Table 2) reinforces the points stated above. For the two dimethyl sulfide compounds whose structures are available the Pt−S and Pt−C^{aromatic} distances are longer for the perchloro complex, but, apart from the expected longer Pt−X bond for the bromo compound (**1a**), the Pt−CH$_3$ and Pt−N bonds have very much the same length for the two derivatives. The deviation from the octahedral geometry around the SMe$_2$ ligand is less pronounced for **1e**, indicating a lesser degree of strain in the complex.

(17) (a) Tolman, C. A. *Chem. Rev.* **1977**, *77*, 313. (b) Martinez, M.; Muller, G. *J. Chem. Soc., Dalton Trans.* **1989**, 1669. (c) Brown, T. L.; Lee, K. J. *Coord. Chem. Rev.* **1993**, *128*, 89.

(18) (a) Isaacs, N. S. *Physical Organic Chemistry*, 2nd ed.; Wiley: New York, 1995. (b) Pipoh, R.; van Eldik, R.; Henkel, G. *Organometallics* **1993**, *12*, 2236.

(19) Crispini, A.; Ghedini, M. *J. Chem. Soc., Dalton Trans.* **1997**, 75.

It seems that the weaker σ-donor character of the perchloro metalated ring and that of the X ligand produces a slight overall decrease in the strain of the molecule as found in many other systems.[20] Summarizing, although the two available crystal structures of the compounds studied do not differ greatly, their differences correlate with the lesser degree of dissociativeness for substitution reactions of complex **1e** when compared with **1a**. The strain on the molecule as well as the longer Pt−S bond distance enables a lesser degree of dissociation in the transition state of the reaction for compound **1e**. As for the structure of the dinuclear compound **1f2**, Pt−Br bond distances and X−Pt−C angles in Table 2 indicate the unsymmetrical nature of the $\{Pt_2-Br_2\}$ central core of the dimer, as detected via ^{1}H NMR, where four methyl, two C*H*, and two CH_2 resonances are present. Although the bond distances and angles are not relevant for the substitution reactions discussion, the fact that this dinuclear compound is obtained from **1f** on standing is compelling evidence for the formation of a very labile pentacoordinated species $\{Pt(C\frown N)(CH_3)_2Br\}$ in solution. Unfortunately, its concentration is kept very low by an unfavorable equilibrium constant K_1, not allowing its detection by NMR. Only further favorable reaction with phosphines or precipitation as **1f2** reveals its presence.

Finally, with respect to the k_{-1}/k_2 ratios measured for the substitution processes studied, the errors involved in the method used for its determination (see below) have to be considered, and any discussion should be *extremely* cautious. The values are calculated from the double-reciprocal plots of the rate law (eq 6, Scheme 2), as that shown in Figure 3 (k_{-1}/k_2 = slope/intercept). The fact that slopes are high and intercepts very small produces values with very large statistical errors. Despite this fact, the values found for the temperature averaged k_{-1}/k_2 ratios for the compounds studied, and collected in Table 5 as a function of the phosphine ligands and solvents, seem to be rather indicative of the process taking place on the pentacoordinate intermediate of the substitution reaction. For most of the compounds, the values are greater than or equal to unity, indicating a general preference of the lower coordination number intermediate for the SMe_2 ligand with respect to the substituting phosphine. Nevertheless, this preference is reduced for the complex having the most electron-withdrawing ligand, **1e**, but for the Pt^{IV} center with the most rigid dangling arm, **1f**, the preference is increased. Given the fact that the differences in hardness between the dimethyl sulfide and phosphine ligands is small, the general preference has to be related to the different bulkiness of the phosphine and dimethyl sulfide ligands. In this respect, a tuning of the values of the ratio is insinuated when the cone angles, θ, are considered; the bulkier the phosphine, the more difficult its relative entrance on the pentacoordinate intermediate depicted in Scheme 2. Furthermore, no clear trend on the pK_a values for the different phosphines is detected, which seems to indicate that the steric tuning could be the dominant factor for the reactivity observed. Anyway, as stated before, the large errors involved do not allow any further comments.

(20) Comba, P. *Coord. Chem. Rev.* **1992**, *182*, 343.

Table 5. Values of the Rate Constants Ratio k_{-1}/k_2 Averaged for Different Solvents at Temperatures for the Substitution Reactions of the Systems Studied[a]

compound	phosphine	solvent	k_{-1}/k_2
1a	χ	acetone	3.1
		chloroform	3.9
		toluene	3.5
	ϵ	acetone	4.9
		toluene	5.0
1b	α	acetone	1.6
	χ	acetone	2.0
		chloroform	2.1
	ϵ	acetone	2.9
1c	α	acetone	2.3
	β	acetone	2.3
	χ	acetone	3.1
	δ	acetone	3.3
	ϵ	acetone	3.9
	ϕ	acetone	3.9
1e	χ	acetone	0.79
		chloroform	1.1
	ϵ	acetone	0.99
		chloroform	1.6
1f	χ	acetone	6.3
	ϵ	acetone	9.7

[a] From ref 17a: $PMePh_2$, α, pK_a = 4.06, θ = 136°. $PEtPh_2$, β, pK_a = 4.6, θ = 140°; PPh_3, χ, pK_a = 3.28, θ = 145°; $P(4\text{-}MeC_6H_4)_3$, δ, pK_a = 4.46, θ = 145°; $P(3\text{-}MeC_6H_4)_3$, ϵ, pK_a = 4.7, θ = 165°; PCy_3, ϕ, pK_a = 11.26, θ = 170°.

Experimental Section

Instruments. ^{1}H NMR spectra were recorded with Varian XL-200 (200 MHz) and Varian XL-300 (300 MHz) spectrometers, while ^{31}P{^{1}H} NMR spectra were obtained by using a Bruker 250 DRX (101.25 MHz) spectrometer. Chemical shifts (in ppm) were measured relative to $SiMe_4$ for ^{1}H and to 85% H_3PO_4 for ^{31}P spectra; the solvent used was acetone-d_6.

Products. All the phosphine ligands used in this study were used as commercially available; solvents were distilled and keep under N_2. All complexes have been prepared according to the established literature procedures.[10] Compounds **1a**, **1c**, **1e**, and **1f** have been characterized via ^{1}H NMR spectra, in all cases very good agreement with previously reported values is obtained. For compound **1b** the general synthetic procedure is the same as that described for the other complexes;[10] imine **b** was prepared via condensation of the 2Br-benzaldehyde, and the corresponding amine which was prepared from the sodium reduction of mesitylnitrile[21a] obtained from the corresponding aldehyde using a published procedure.[21b] Spectroscopic data agree with the proposed formulation (^{1}H NMR; δ/ppm(J/Hz): 1.08(^2J(Pt−H) 71) 3H(Me), 1.30(^2J(Pt−H) 68) 3H(Me), 2.10(^2J(Pt−H) 14) 6H(SMe_2), 5.21/5.42 (^2J(H−H) 19) 2H(CH), 7.89(^3J(Pt−H) 46) 1H(CH)). Compound **1f2** has been obtained after prolonged periods of standing of compound **1f** in acetone solution. Spectroscopic data agree with the proposed formulation (^{1}H NMR in $CDCl_3$; δ/ppm(J/Hz): 1.24(^2J(Pt−H) 78) 3H(Me), 1.33(^2J(Pt−H) 78) 3H(Me), 1.86(^2J(Pt−H) 73) 3H(Me), 2.06(^2J(Pt−H) 73) 3H(Me), 4.10/4.76(^2J(H−H) 15) 2H(CH_2), 4.72/4.90(^2J(H−H) 15) 2H($_{CH}$), 8.47(^3J(Pt−H) 24) 1H(CH), 8.94(^3J(Pt−H) 25) 1H(CH)). For the phosphine derivatives the standard published procedure[10] has been also applied; characterization of the complexes has been achieved via ^{31}P and ^{1}H NMR spectra. Table S16 (Supporting Information) collects all the characterization NMR data from both the literature and the new compounds studied.

Crystallography. Good quality X-ray crystals from compounds **1a**, **1e**, and **1f2** were obtained by cooling concentrated

(21) (a) Lawrance, G. A.; Martinez, M.; Skelton, B. W.; White, A. H. *J. Chem. Soc., Dalton Trans.* **1992**, 1649. (b) Kumar, H. M. S.; Reddy, B. V. S.; Reddy, P. T.; Yadav, J. S. *Synthesis* **1999**, 586.

acetone solutions of each complex in a refrigerator for extended periods. Intensity data for the compounds were measured on an Enraf-Nonius CAD4 four-circle diffractometer using graphite-monochromated Mo Kα radiation (λ 0.71073 Å) in the $\omega-2\theta$ scan mode. Lattice dimensions were determined by a least-squares fit of the setting parameters of 25 independent reflections. Data reduction and empirical absorption corrections were performed with the XTAL package.[22] Structures were solved by heavy-atom methods with SHELXS-86[23] and refined by full-matrix least-squares analysis with SHELXL97.[24] All non-H atoms were refined with anisotropic thermal parameters. Crystallographic data are given in Table 1, and selected bond lengths appear in Table 2. The atomic nomenclature is defined in Figure 1, drawn with the graphics program PLATON.[25]

Kinetics. The reactions were followed by UV−vis spectroscopy in the 500−340 nm range, where none of the solvents absorb. Runs with $t_{1/2} > 170$ s were recorded on an HP8452A instrument equipped with a thermostated multicell transport; runs within the 7−170 s margin were recorded on a HP8452A or a J&M TIDAS instrument and using a High-Tech SFA-11 Rapid Kinetics Accessory; for $t_{1/2} < 7$ s a Durrum D-110 stopped-flow instrument connected to a J&M TIDAS spectrophotometer was used. Observed rate constants were derived from absorbance versus time traces at the wavelengths where a maximum increase and/or decrease of absorbance was observed. Table S12 (Supporting Information) collects all the obtained k_{obs} values for all the complexes studied as a function of the starting complex, entering phosphine ligand, and temperature. No dependence of the observed rate constant values on the selected wavelengths was detected, as expected for reactions where a good retention of isosbestic points is observed. The general kinetic technique is that previously described.[10,26] In all cases pseudo-first-order conditions were maintained and the platinum concentration was maintained at 2.5×10^{-4} M to avoid undesired decomposition reactions.

Acknowledgment. We acknowledge financial support for the PB97-0914 project from the Ministerio de Educación y Cultura.

Supporting Information Available: Listing of the crystal structure data for compounds **1a**, **1e**, and **1f2**, NMR data for the compounds **2** prepared in this study, and observed rate constants for the reactions studied. This material is available free of charge via the Internet at http://pubs.acs.org.

OM000505Y

(22) Hall, S. R., Flack, H. D., Stewart, J. M., Eds. *The XTAL3.2 User's Manual;* Universities of Western Australia: Geneva and Maryland, 1992.
(23) Sheldrick, G. M. *Acta Crystallogr.* **1990**, *A46*, 467.
(24) Sheldrick, G. M. *SHELXL97, Program for Crystal Structure Determination;* University of Göttingen, 1997.
(25) Spek, A. L. *Acta Crystallogr.* **1990**, *A46*, C34.
(26) Martinez, M.; Pitarque, M.-A.; van Eldik, R. *J. Chem. Soc., Dalton Trans.* **1994**, 3159.